Nuclear Physics B173 (1980) 77–92

GENERAL FEATURES OF THE $\bar{p}p$ INTERACTION AT 12 GeV/c

P. JOHNSON, P. MASON, H. MUIRHEAD, P. MICHAELIDES[1], CH. MICHAELIDOU[1] and G.D. PATEL

Department of Physics, University of Liverpool, UK

G.W. VAN APELDOORN, D. HARTING, D. J. HOLTHUIZEN, J.M. DE LEEUW, B.J. PIJLGROMS and M.M H M. RIJSSENBECK

NIKHEF-H, Amsterdam, The Netherlands

V. KARIMAKI, M. KORKEA-AHO, R. KINNUNEN and J. TUOMINIEMI

Department of High Energy Physics, University of Helsinki, Finland

G. EKSPONG, T. MOA and S. NILSSON

Institute of Physics, University of Stockholm, Sweden

Received 7 February 1980

Simple inclusive cross sections for $\bar{p}p$ interactions at 12 GeV/c are given. The data cover prong cross sections, V^0 production and resonances. Separation has been made into annihilation and non-annihilation modes. Some implications of the data are discussed. It is pointed out that the ratios of cross sections for ρ^0/π^- production are independent of incident antiproton momentum in $\bar{p}p$ annihilation processes, and that data at the highest available pp energies (ISR) tend to the same value.

1. Introduction

In this paper we present some data on the general features of the $\bar{p}p$ interaction at 12 GeV/c. The experiment was performed in the CERN 2 m HBC. Measurements on all topologies were carried out on the measuring machines at our institutes (FSD's-Amsterdam and Liverpool, Sweepnik-Helsinki, Spiral Reader-Stockholm). The results given in this report are from samples of 99 125 events of all categories and 4382 V^0 events.

In sect. 2, topological cross sections are given and compared with pp data at 12 GeV/c. Data on the yields of V^0 particles (K^0_S, Λ, γ) are presented in sect. 3, and differential properties in sect. 4. Inclusive information on the more commonly

[1] Permanent address. Laboratory of Nuclear Physics, University of Athens, Greece.

TABLE 1
Topological cross sections (mb) at 12 GeV/c

σ_n	$\bar{p}p$ (this expt.)	pp (ref. [2])	Difference	Annihilation
σ_0	1.26 ± 0.1		1.26 ± 0.1	
$\sigma_{2\,\mathrm{inel}}$	12.31 ± 0.2	12.70 ± 0.25	-0.39 ± 0.3	1.2 ± 0.4
σ_4	16.02 ± 0.15	13.20 ± 0.10	2.82 ± 0.2	3.7 ± 0.4
σ_6	7.86 ± 0.09	3.45 ± 0.04	4.41 ± 0.1	5.1 ± 0.2
σ_8	2.41 ± 0.04	0.381 ± 0.013	2.03 ± 0.04	2.1 ± 0.1
σ_{10}	$0\,45 \pm 0.02$	0.013 ± 0.002	0.44 ± 0.02	0.44 ± 0.03
σ_{12}	0.046 ± 0.01		0.046 ± 0.01	0.046 ± 0.01
σ_{14}	0.003 ± 0.001		0.003 ± 0.001	0.003 ± 0.001
σ_{inel}	40.36 ± 0.1	29.75 ± 0.25	10.6 ± 1.0	
σ_{el}	11.34 ± 0.6	9.85 ± 0.20	1.5 ± 0.6	
σ_{tot}	51.7 ± 0.8	39.6 ± 0.1	12.1 ± 0.8	12.59 ± 0.6

occurring resonances ($\rho, \omega, \Delta^{++}$, K* and Σ*) is given in sect. 5. Where appropriate, comparisons have been made with other work in pp and $\bar{p}p$ interactions at 12 GeV/c; in addition separation into annihilating and non-annihilating components has been made. Some concluding remarks are made in sect. 6.

2. Inclusive proton and pion cross sections

Table 1 gives the topological cross sections σ_n for the various charged particle multiplicities n. Substantial agreement was obtained between all four participating laboratories and so only the mean values are presented. The errors contain statistical uncertainties as well as systematic normalization uncertainties. The elastic cross section, σ_{el}, involved an extrapolation to t (four-momentum transfer squared) equal to zero. Absolute cross sections were obtained by normalising the total number of events to a value $\sigma_{\mathrm{tot}} = 51.7 \pm 0.8$ mb, obtained by interpolating information from the CERN-HERA data tables*.

The values given in table 1 are in good overall agreement with those reported by Gall [1] in a small statistics $\bar{p}p$ experiment at 12 GeV/c. We also include in table 1 data on pp reactions at 12 GeV/c [2], together with differences in cross sections. It is apparent that the differences are most significant for the higher multiplicities, and can be basically attributed to the annihilation component in $\bar{p}p$ interactions [3]. As a cross check on this conclusion we have separated our $\bar{p}p$ data into annihilating and non-annihilating components using the techniques developed by Gregory [4]. The results for annihilation are presented in the final column of table 1. It can be seen that substantial agreement exists between (a) the difference of $\bar{p}p$

* An independent check on this number has been made by considering the distribution of events along the length of the chamber. After corrections for a small π^- contamination a cross section of 51.0 ± 1.6 mb was obtained.

TABLE 2
Comparison of inclusive proton and meson cross sections (mb) obtained by use of the boost and Gregory techniques

	σ(proton)		$\sigma(\pi^+)$	
σ_n	Boost	Gregory	Boost	Gregory
$\sigma_{2\,\mathrm{inel}}$	5.15 ± 0.09	5.40 ± 0.5	6.96 ± 0.08	6.7 ± 0.5
σ_4	8.89 ± 0.11	8.39 ± 0.5	23 17 ± 0.12	23.3 ± 0.5
σ_6	2.69 ± 0.07	2.37 ± 0.15	20.86 ± 0.09	21.0 ± 0.3
σ_8	0.30 ± 0.04	0.27 ± 0.03	9.34 ± 0.06	9.35 ± 0.2
σ_{10}	0.016 ± 0.016	0.010 ± 0.010	2.28 ± 0.03	2.28 ± 0.1
σ_{12}			0.27 ± 0.01	0.27 ± 0.01
Total	17.04 ± 0.16	16.44 ± 0.7	62.86 ± 0.18	62.91 ± 0.8

and pp cross sections and the annihilation cross sections and (b), by implication, the pp and non-annihilation cross sections. A further check on the separation technique of Gregory has been performed; the latter works on an event by event basis and thus it is possible to obtain the inclusive cross section for protons and pions in the total sample. Overall separation into protons and pions may also be achieved by a technique [5, 6] involving Lorentz boosts and reflections as described in the appendix. In table 2 the inclusive cross sections for protons and π^+ mesons are compared for the two methods and it is apparent that overall agreement has been achieved. A variant of the Lorentz boost technique has also been applied to pp data at 12 GeV/c [6] and the proton yields are found to be essentially twice those given in columns 2 and 3 of table 2. It should be noted that the sums of the cross sections for proton and π^+ meson by the two methods do not agree exactly in table 2. This is because some identification of kaons has been made in making the separation (of Gregory) into annihilation and non-annihilation processes.

3. V^0 cross sections

V^0 events have been recorded in this experiment and 3-constraint reconstructions made in order to search for the reactions

$$\bar{p}p \rightarrow K^0_S X,$$

$$\bar{p}p \rightarrow (\Lambda/\bar{\Lambda})X,$$

$$\bar{p}p \rightarrow \gamma X.$$

All film has been double scanned for V^0 events and small corrections made for scanning efficiency (98%). Corrections were made for (a) loss of V^0 produced close to the primary vertex or outside the chamber, (b) loss of events during measurements and data reduction.

TABLE 3
Comparison of V^0 cross sections (mb) for $\bar{p}p$, pp at 12 GeV/c

	$\sigma(K_S^0)$	$\sigma(\Lambda)$	$\sigma(\bar{\Lambda})$	$\sigma(\gamma)$
$\bar{p}p$ (this expt)	2.15 ± 0.20	1.18 ± 0 07	1.0 ± 0.10	141 ± 6
$\bar{p}p$ (ref. [7])	2.14 ± 0 19	1.24 ± 0.11	1.14 ± 0 11	
$\bar{p}p$ (ref. [1])	1 85 ± 0.06	0.91 ± 0.05		
pp (ref. [2])	0.575 ± 0.02	1.12 ± 0.04	0.002 ± 0.001	70.4 ± 4.8
pp (ref. [8])	0.685 ± 0.08	1.07 ± 0.11		63.1 ± 5.1

Two well-known problems in data reduction of this nature have been encountered by us, namely losses of γ events corresponding to π^0 moving backwards in the c-system, and the "disappearance" of $\bar{\Lambda}$ events (the cross sections for Λ and $\bar{\Lambda}$ production should be equal for $\bar{p}p$ reactions from charge conjugation invariance). We have therefore used only data for γ moving forwards in the c-system and doubled our values, and have concentrated on Λ events when discussing physical problems. Again substantial agreement was achieved between the measurements in the individual laboratories and so only mean values are reported.

In table 3, we present our total cross sections and compare them with other $\bar{p}p$ and pp reactions at 12 GeV/c. The K_S^0 and Λ cross sections have been corrected for unseen decay modes. Reasonable agreement with other $\bar{p}p$ experiments has been achieved [1, 7]. It can be seen that the inclusive cross sections are considerably bigger for K_S^0 and γ production in $\bar{p}p$ than pp [2, 8]; this excess can be expected to arise from the annihilation component. However, it is also apparent that the cross sections for Λ and $\bar{\Lambda}$ production differ considerably for $\bar{p}p$ and pp reactions. The differences may be attributed to the baryon numbers $B = 0$ and 2 for the $\bar{p}p$ and pp systems respectively. Thus in table 3 the difference in cross sections for $\bar{p}p \to \Lambda X$ and one half $pp \to \Lambda X$ (allowing for two initial protons) is 0.62 ± 0.11 mb, whereas we find the measured cross section for $\bar{p}p \to \bar{\Lambda}\Lambda X$ to be 0.53 ± 0.1 mb. Consultation of table 3 indicates that $pp \to \bar{\Lambda}\Lambda X$ must be negligible at 12 GeV/c.

In tables 4 and 5 the topological cross sections for K_S^0 and Λ production* for $\bar{p}p$ and pp reactions are compared and differences taken for suitable combinations (see footnote to table 4). The Λ difference (table 4), which we believe to be mainly $\bar{p}p \to \bar{\Lambda}\Lambda X$, is seen to concentrate in channels of low multiplicity. On the other hand the K_S^0 difference (table 5) indicates substantial differences up to the eight-prong channel, thus suggesting that the difference mainly arises in the

* Our topological cross sections for these channels are in substantial agreement with those in ref. [7].

TABLE 4
Topological cross section (mb) for $\sigma(\bar{p}p \to \Lambda X)$ and $\frac{1}{2}\sigma(pp \to \Lambda X)$[a] and differences

σ_n	$\bar{p}p$ (this expt.)	$\frac{1}{2}$(pp) (ref. [8])	Difference
σ_0	0.20 ± 0.04		0.20 ± 0.04
σ_2	$0.64 \pm 0\,05$	0.325 ± 0.05	0.31 ± 0.07
σ_4	0.30 ± 0.03	$0\,180 \pm 0.03$	0.12 ± 0.05
σ_6	0.04 ± 0.01	0.028 ± 0.005	0.01 ± 0.01
σ_8		0.002 ± 0.002	
σ_{tot}	1.18 ± 0.07	0.535 ± 0.05	0.64 ± 0.11

[a] A factor of $\frac{1}{2}$ has been introduced to compensate for two protons in the initial state.

annihilation channels. We have again checked this assumption using the techniques of Gregory [4] and the results are displayed in table 5. Again we may make the same comments as for table 1 regarding the success of this approach.

We have used the data of tables 1 and 5 to establish the proportion of annihilation events containing K^0_S mesons as a function of prong number. Both ($\bar{p}p$, pp) differences and the method of Gregory have been applied and the results are given in table 6. Bearing in mind that equal numbers of K^0_L mesons are being produced, then this table indicates substantial production of strange mesons in the $\bar{p}p$ annihilation at 12 GeV/c especially in the channels of lower multiplicity. The fall-off in the ratio at higher multiplicities can be anticipated from the influence of phase space.

Topological cross sections for $\bar{p}p \to \pi^0 X$ and $pp \to \pi^0 X$ are given in table 7, together with their differences (since virtually all the γ-rays arise from π^0 decay the cross sections for π^0 production represent essentially half those for γ production). It can be seen that the difference follows the general trend of the differences in table 1 and is indicative of the strong contribution of the annihilation component to the $\bar{p}p$ data to the events of high charged multiplicity. This conclusion is again

TABLE 5
Topological cross sections (mb) for $\sigma_n(\bar{p}p/pp \to K^0_S X)$ and differences

σ_n	$\bar{p}p$ (this expt.)	pp (ref. [8])	Difference	Annihilation
σ_0	0.15 ± 0.04		0.15 ± 0.04	0.10 ± 0.04[a]
σ_2	0.66 ± 0.1	0.35 ± 0.06	0.31 ± 0.12	0.15 ± 0.04
σ_4	$0.84 \pm 0\,13$	0.29 ± 0.05	$0.55 \pm 0\,14$	0.47 ± 0.05
σ_6	0.42 ± 0.06	0.05 ± 0.02	0.37 ± 0.06	0.40 ± 0.04
σ_8	$0\,08 \pm 0.02$	$0\,003 \pm 0.003$	0.08 ± 0.02	0.08 ± 0.02
σ_{tot}	2.15 ± 0.15	0.69 ± 0.08	1.46 ± 0.2	1.20 ± 0.1[a]

[a] This figure represents an upper limit. Since we are unable to apply the separation technique to zero-prong events, we have removed all those events containing a Λ or $\bar{\Lambda}$ associated with K^0_S.

TABLE 6
Proportion of annihilation events containing a K^0_S

Prong number	($\bar{p}p$, pp) differences	Annihilation
0	0.14 ± 0.03	
2		0.14 ± 0.06
4	0.19 ± 0.04	0.13 ± 0.02
6	0.08 ± 0.02	0.08 ± 0.01
8	0.04 ± 0.01	0.04 ± 0.01

TABLE 7
Topological cross sections (mb) for $\sigma_n(\bar{p}p/pp \to \pi^0 X_n)$ and differences

σ_n	$\bar{p}p$ (this expt.)	pp (ref. [1])	Difference	Annihilation
σ_0	3.0 ± 0.5		3.0 ± 0.5	
σ_2	22 ± 3	15.8 ± 2	6.2 ± 3.5	1.6 ± 3
σ_4	26 ± 3	15.0 ± 1.5	11.0 ± 3.5	6.1 ± 3
σ_6	15 ± 2	4.2 ± 0.6	10.8 ± 2	10.7 ± 2
σ_8	$4\,5 \pm 1$	0.3 ± 0.06	4.2 ± 1	4.5 ± 1
σ_{tot}	70.5 ± 3	35.3 ± 3.0	35.2 ± 5	22.9 ± 5

reinforced using the method of Gregory [4] and the relevant results are also displayed in table 7.

4. Differential distributions for V^0

In figs. 1 and 2, we display the data for the distributions*

$$F(x) = \frac{1}{\pi p^*_{L\,max}} \int \frac{E^* \, d^2\sigma}{dx \, dp_T^2} \, dp_T^2 \tag{1}$$

and

$$d\sigma/dp_T^2$$

for K^0_S, Λ and γ particles. They agree substantially with the results of ref. [7]. It is evident from fig. 1 that Λ production is highly peripheral compared with K^0_S or γ production.

Comparisons with pp data are made in figs. 3 and 4. In the former diagram we display $F(x)$ for $\bar{p}p \to \Lambda X$ and also the sum $\bar{p}p \to \Lambda X$ and its reflection corresponding to $\bar{p}p \to \bar{\Lambda} X$; the sum is indicated by the dashed line whilst the data for

* As usual x and p_T refer to the Feynman variables.

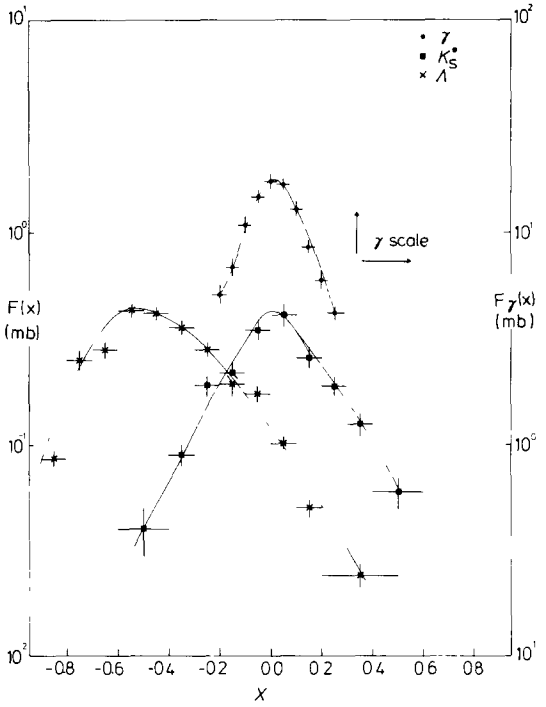

Fig. 1. Distributions of the invariant cross section

$$F(x) = \frac{1}{\pi p^*_{\mathrm{L\,max}}} \int \frac{E^* \mathrm{d}^2\sigma}{\mathrm{d}x\,\mathrm{d}p_\mathrm{T}^2}\,\mathrm{d}p_\mathrm{T}^2$$

as a function of x for V^0 particles. Data include branching ratios for K_S^0 and Λ.

$pp \to \Lambda X$ at 12 GeV/c [2] are given by the dotted line. It is apparent that a substantial difference between $\bar{p}p$ and pp data occurs near $|x| \to 1$; this difference can be associated with $\bar{p}p \to \bar{\Lambda}\Lambda X$, which we can expect to be mainly peripheral and of low multiplicity as indicated in table 4. In fig. 4 we show $\mathrm{d}\sigma/\mathrm{d}p_\mathrm{T}^2$ for the annihilation and non-annihilation components of K_S^0, together with the trend of the pp data. It is apparent that $\mathrm{d}\sigma/\mathrm{d}p_\mathrm{T}^2$ for the non-annihilation component and pp are virtually identical in slope and absolute magnitude, as might be expected. It can also be seen that the distribution is much flatter for the annihilation component. Finally in fig. 5 we show average transverse momentum, $\langle p_\mathrm{T} \rangle$, as a function of x for the annihilation and non-annihilation components. It is evident that K_S^0 mesons originating in non-annihilation processes are more centrally produced and have lower $\langle p_\mathrm{T} \rangle$ than in annihilation processes. This behaviour reflects the fact that a K_S^0 meson can assume the rôle of a leading particle in an annihilation reaction, but not in a non-annihilation process.

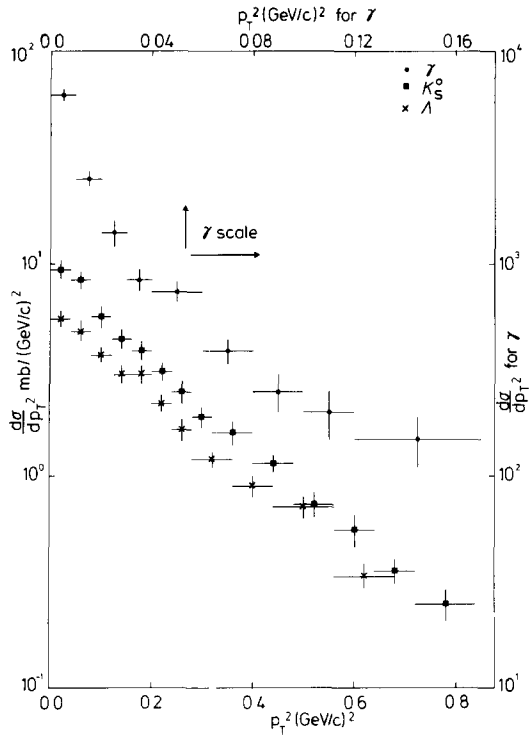

Fig. 2. $d\sigma/dp_T^2$ for V^0 events.

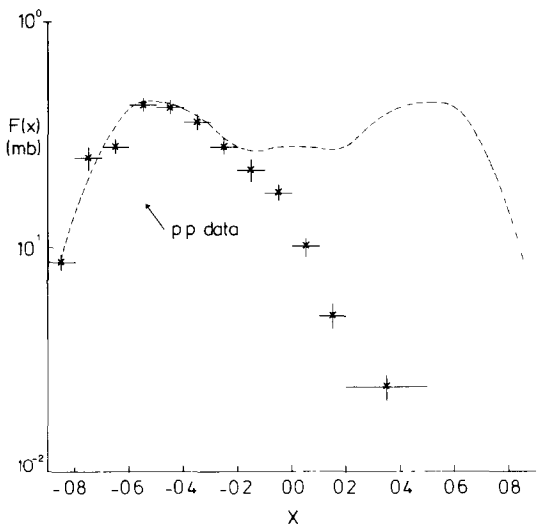

Fig 3 Trends of $F(x)$ for $\bar{p}p \rightarrow \Lambda x$ (crosses) plus reflected data (dashes) compared with $F(x)$ for $pp \rightarrow \Lambda x$ (dotted line).

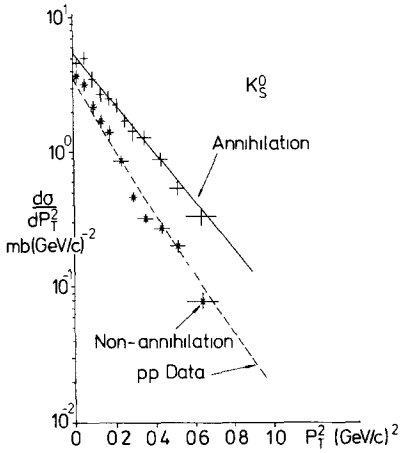

Fig. 4. $d\sigma/dp_T^2$ for $\bar{p}p \to K^0_S X$ for annihilation and non-annihilation data. The dashed line gives the trend of the corresponding pp data. The solid line represents the fit $d\sigma/dp_T = A\exp(-bp_T^2)$ with $A = 5.13 \pm 0.08$ mb $(GeV/c)^{-2}$ and $b = 4.13 \pm 0.63$ $(GeV/c)^{-2}$.

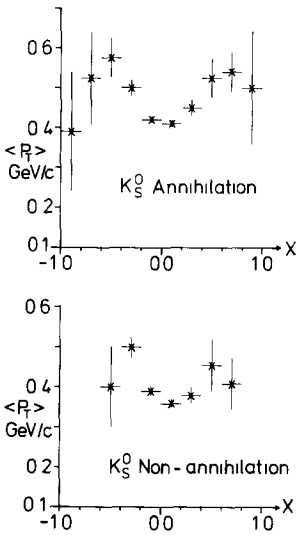

Fig. 5. Average $\langle p_T \rangle$ versus x for K^0_S for annihilation and non-annihilation data.

5. Resonance production

Inclusive cross sections for the more commonly occurring resonant states have been measured by us. The measurements were based on mass distributions for $\pi^+\pi^-(\rho^0, \omega)$, $p\pi^+(\Delta^{++})$, $K^0_S\pi^\pm(K^*(892))$ and $\Lambda\pi^\pm(\Sigma^*(1385))$. In ref. [9] it has been argued that the ω cross section can be deduced from the $\pi^+\pi^-$ mass distribution by exploiting the properties of the matrix element for ω decay. Typical

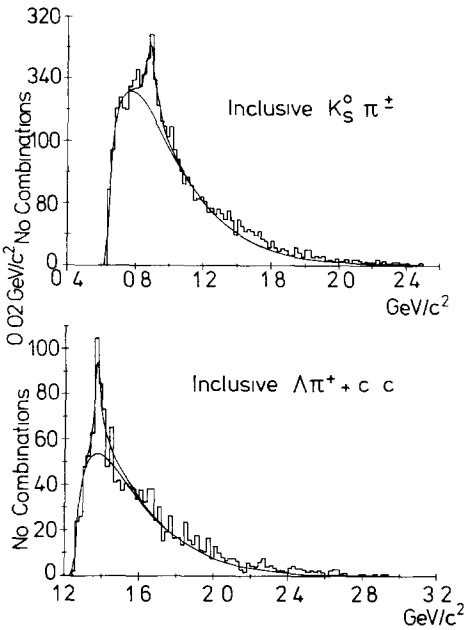

Fig. 6. Sample plots used in resonance fitting.

examples of the data available to us are shown in fig. 6 where $K^0_S\pi^\pm$ and $\Lambda\pi^+$ (plus charge conjugate) combinations are displayed. Fits of the form

$$\frac{d\sigma}{dM} = BG(1 - f + f\,BW),$$

where M = mass combination, BG = background, f = fraction of combination in resonance, BW = Breit-Wigner or suitable resonance parametrisation were made to the data, and cross sections are given in table 8 (corrected for unseen decay modes). The values given in this table show satisfactory agreement with the values

TABLE 8
Inclusive resonance cross sections (mb)

	ρ^0	ω	f	$K^{*\pm}(892)$[a]
Inclusive	6.78 ± 0.15	7.45 ± 0.20	1.92 ± 0.10	0.95 ± 0.10
Annihilation	4.99 ± 0.25	5.01 ± 0.30	0.69 ± 0.15	0.69 ± 0.08
Non-annihilation	2 11 ± 0.15	2.55 ± 0.15	0.89 ± 0.15	

	Δ^{++} + c.c.	Σ^{*-} + c.c.	Σ^{*+} + c.c.
Inclusive	5.59 ± 0.56	0.16 ± 0.03	0.28 ± 0.03

[a] $K^{*\pm}$ refers to the sum of + and − states.

for resonances reported in refs. [1, 10]; values for ρ^0 and f production have already been reported by this collaboration [11] using a different approach to the estimation of background—the results are in substantial agreement. In addition we have also split our data into components for annihilation and non-annihilation; the appropriate cross sections are also given in table 8. The apparent failure of the annihilation and non-annihilation components to sum to the inclusive cross sections arises because independent determinations were made for each sample.

6. Discussion

Several conclusions may be drawn from the data presented in the preceding sections:

(1) Despite the fact that charge conjugate baryon states ($\bar{p}p \to \bar{Y}YX$, $\bar{p}p \to \bar{\Delta}\Delta$, etc.) are possible in $\bar{p}p$ but not in pp reactions the main features of the annihilation processes appear to be essentially equal to the appropriate differences of $\bar{p}p$ and pp processes at 12 GeV/c.

(2) The charge conjugate nature of the $\bar{p}p$ system leads to substantial differences in Λ production in $\bar{p}p$ and pp reactions (fig. 3).

(3) The average transverse momentum of the kaons in annihilations is higher than in non-annihilations (fig. 4), as already found for pions.

(4) The kaon yield is substantial in annihilation compared with non-annihilation processes. If we take the figure of $2\sigma(K^0_S)$ as a measure of K^0 plus $\bar{K}^0$ production then the appropriate ratios of $2\sigma(K^0_S)$ to the total annihilation and inelastic $\bar{p}p$ cross sections are 0.19 ± 0.02 and 0.046 ± 0.006 respectively.

(5) The yield of kaons relative to pions increases with antiproton momentum in $\bar{p}p$ annihilations. Thus the ratio $2K^0_S/\pi^-$ is 0.042 ± 0.002 and 0.069 ± 0.004 at 0.76 GeV/c [12] and 12 GeV/c respectively*. A similar situation also apparently exists for vector mesons—the ratio $K^{*\pm}/\rho^0$ changes from 0.097 ± 0.005 to 0.14 ± 0.02 in going from 0.76 to 12 GeV/c. On the other hand, the ratios of vector to scalar meson production appear to be independent of energy in antiproton annihilation. The data in table 8 imply ratios for inclusive cross sections of 0.20 ± 0.03 and 0.29 ± 0.04 for ρ^0/π^- and $K^{*\pm}(892)/2K^0_S$, respectively. Data for ρ^0/π^- as a function of energy in the c-system are plotted in fig. 7 [13]; in addition information from pp interactions are also given [2, 14]. It is apparent that the ratios for pp interactions at ISR energies have settled to the same value of $\sim$0.15 which we find in $\bar{p}p$ annihilation from near threshold onwards. Such a result might appear to be plausible since most of the meson production occurs in the central region of high energy pp collisions. The quasi-fireball in this region could then be equivalent to the situation in $\bar{p}p$ annihilation. The situation for $K^*/2K^0_S$ is less clear since the data are more sparse. They are summarised in table 9 [15]. Whilst the figures

* An inclusive cross section of 34.8 ± 1.2 mb for $\bar{p}p \to \pi^-$ plus anything (annihilation) may be deduced from column 5 of table 1.

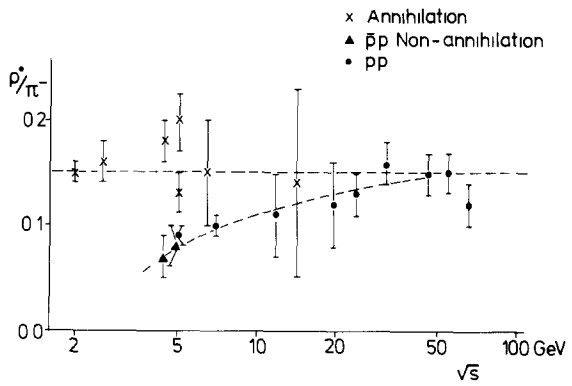

Fig. 7. Ratio of cross sections for inclusive ρ^0/π^- production as function of the energy in the c-system.

TABLE 9
$K^{*\pm}/2K_S^0$ for $\bar{p}p$ and pp reactions

Beam particle	Momentum (GeV/c)	$K^{*\pm}/2K_S^0$ annihilation	$K^{*\pm}/2K_S^0$ non-annihilation, pp
$\bar{p}$	0.76	0.36 ± 0.01	
$\bar{p}$	3.6	0.36 ± 0.01	
$\bar{p}$	12	0.29 ± 0.04	0.14 ± 0.07
$\bar{p}$	12 [1]	$0\ 19 \pm 0\ 06$	0.18 ± 0.09
p	12		0.22 ± 0.03 (K^{*+})
			0.017 ± 0.017 (K^{*-})
p	24		0.26 ± 0.03 (K^{*+})
			0.056 ± 0.08 (K^{*-})
p	69		$0\ 24 \pm 0.12$ (K^{*+})
			0.23 ± 0.11 (K^{*-})
p	200		0.15 ± 0.08 (K^{*+})
			$0\ 15 \pm 0.08$ (K^{*-})
p	400		0.28 ± 0.06 (K^{*+})
			0.24 ± 0.05 (K^{*-})

suggest K^*/K_S^0 production could be energy independent in $\bar{p}p$ annihilation (and also K^{*+}/K_S^0 in pp reactions), the lack of information at high energies for either $\bar{p}p$ or pp reactions does not allow us to draw any firm conclusions. However, if we regard the K^{*-} presence in pp reactions as indicative of the production of pairs of strange mesons, then the situation with respect to K^* production may not be too dissimilar from that shown in fig. 7.

We wish to thank the staff associated with the CERN 2 m H.B.C. program and our home institutions for their consistent support during the data acquisition stages of this experiment. Grateful thanks are also given to the agencies supporting the high energy physics programs in our respective countries, namely F.O.M. and

Z.W.O. (Amsterdam), Valtion Luonnontieeteellinen Toimikunta (Helsinki), S.R.C. (Liverpool) and N.F.R. (Stockholm). C.M. and P.M. wish to thank the members of the Oliver Lodge Laboratory, Liverpool for the warm and kind hospitality received during their stay.

Appendix

COMPUTATION OF THE INCLUSIVE p, $\bar{p}$, π^+ AND π^- SPECTRA IN $\bar{p}p$ COLLISIONS

The following notes describe a method for deriving p, $\bar{p}$, π^+ and π^- single-particle spectra in $\bar{p}p$ collisions making use of only momentum and charge measurements of particle tracks and neglecting any information on particle identification. The method is based on the fact that the particle spectra of $\bar{p}p$ interactions obey charge conjugation (c.c.) symmetry, i.e., the c.m.s. spectrum of a particle is identical with the reflected c.m.s. spectrum of its antiparticle or, in other words, a particle spectrum in the target (laboratory) frame is identical with the corresponding antiparticle spectrum in the beam frame (sometimes called the antilaboratory frame).

Basically a similar method has been used to compute p and π^+ spectra in pp interactions [5, 6] using the fact that the spectra are forward-backward symmetric. This method, formulated in detail in ref. [6], can be applied as such for computing the sum of $p, \bar{p}$ spectra and the sum of π^+, π^- spectra in $\bar{p}p$ interactions. It is of considerable interest, however, to compute separate p, $\bar{p}$, π^+ and π^- spectra. Below we describe the solution to the problem of how to do the separation.

Following the notation of ref. [6] we define the following transformations acting on the longitudinal momentum q:

$R_p : q \to R_p q$ boost from the target frame to the beam frame or vice versa under the assumption that the track has the proton, antiproton mass, followed by a reflection along the longitudinal momentum axis,

$R_\pi : q \to R_\pi q$ the same as R_p but assuming the pion mass for the track.

The above definitions imply

$$R_p q = -\gamma q + \eta\sqrt{q^2 + r^2 + m_p^2} ,$$

$$R_\pi q = -\gamma q + \eta\sqrt{q^2 + r^2 + m_\pi^2} ,$$

where r^2 is the transverse momentum squared and γ and η are the Lorentz transformation factors

$$\gamma = E_{\text{beam}}/m_p , \qquad \eta = p_{\text{beam}}/m_p .$$

We further split the operations R_p and R_π in two parts, one acting only on the positive tracks and the other on the negative ones:

$$R_p^{(+)}, \qquad R_p^{(-)}, \qquad R_\pi^{(+)}, \qquad R_\pi^{(-)} .$$

It follows from the definition of these operators and from the c.c. symmetry of $\bar{p}p$ interactions that

$$R_p^{(\pm)} d\sigma(\mp) = R_\pi^{(\pm)} d\sigma(\mp) \equiv 0,$$

$$R_p^{(+)} d\sigma(p) = d\sigma(\bar{p}),$$

$$R_p^{(-)} d\sigma(\bar{p}) = d\sigma(p),$$

$$R_\pi^{(\pm)} d\sigma(\pi^\pm) = d\sigma(\pi^\mp).$$

The solution to our problem is now given by the following infinite operator series

$$P_p = I^{(+)} - R_\pi^{(-)} + R_\pi^{(-)} R_p^{(+)} - R_\pi^{(-)} R_p^{(+)} R_\pi^{(-)} + \cdots,$$

$$P_{\bar{p}} = I^{(-)} - R_\pi^{(+)} + R_\pi^{(+)} R_p^{(-)} - R_\pi^{(+)} R_p^{(-)} R_\pi^{(+)} + \cdots,$$

$$P_{\pi^+} = I^{(+)} - R_p^{(-)} + R_p^{(-)} R_\pi^{(+)} - R_p^{(-)} R_\pi^{(+)} R_p^{(-)} + \cdots,$$

$$P_{\pi^-} = I^{(-)} - R_p^{(+)} + R_p^{(+)} R_\pi^{(-)} - R_p^{(+)} R_\pi^{(-)} R_p^{(+)} + \cdots,$$

where $I^{(\pm)}$ is the identity operator: $I^{(\pm)} d\sigma(\pm) = d\sigma(\pm)(I^{(\pm)} d\sigma(\mp) = 0)$. Namely, when we operate with them on the summed spectrum $d\sigma \equiv d\sigma(p + \bar{p} + \pi^+ + \pi^-) \equiv d\sigma(p) + d\sigma(\bar{p}) + d\sigma(\pi^+) + d\sigma(\pi^-)$, we see that separated spectra $d\sigma(p)$, $d\sigma(\bar{p})$, $d\sigma(\pi^+)$ and $d\sigma(\pi^-)$ are extracted.

In order to demonstrate this in more detail, let us take the operator P_p. We first see that

$$P_p d\sigma(p + \bar{p}) = d\sigma(p),$$

because the first term in the series gives $d\sigma(p)$, the second and the third terms cancel, the fourth and the fifth term cancel, and so on. On the other hand,

$$P_p d\sigma(\pi^+ + \pi^-) = 0,$$

because the first and second terms cancel, and so on. Hence indeed

$$P_p d\sigma(p + \bar{p} + \pi^+ + \pi^-) = d\sigma(p).$$

The infinite series above are convergent in the sense that the higher-order terms, when operating on a given spectrum, approach a zero density distribution. This follows from the inequalities

$$R_\pi R_p q < q < R_p R_\pi q,$$

which hold for all r and q. This means that the range of a distribution like $R_\pi R_p \cdots R_\pi R_p \, d\sigma$ increases as a function of the number of repeated operations R, implying a decrease in the density. In practice one has to compute only those transformed longitudinal momenta (e.g., $R_\pi^{(-)} R_p^{(+)} R_\pi^{(-)} q$ which build up the partial spectrum $R_\pi^{(-)} R_p^{(+)} R_\pi^{(-)} d\sigma$ in the series expansion) which remain inside the kinematically allowed region. On the average about 5 terms were enough and the practical upper limit was 17 in our computation.

In practice it turns out that the spectra $d\sigma(p)$ and $d\sigma(\bar{p})$ derived by the above operators are statistically inaccurate in the backward hemisphere, the same being true for the spectra $d\sigma(\pi^+)$ and $d\sigma(\pi^-)$ in the forward hemisphere. This situation is reversed, if the following operators are used:

$$P'_p = R_p^{(-)} P_{\bar{p}}, \qquad P'_{\bar{p}} = R_p^{(+)} P_p,$$

$$P'_{\pi^+} = R_\pi^{(-)} P_{\pi^-}, \qquad P'_{\pi^-} = R_\pi^{(+)} P_{\pi^+}.$$

The operators P and P' define two different methods to compute the spectra. Therefore, a suitably weighted combination of the two operators will give a statistically more accurate result. Hence we compute the spectra as follows:

$$d\sigma(p) = \left\{ W(X_p) P_p + \left[1 - W(X_p) \right] P'_p \right\} d\sigma,$$

$$d\sigma(\pi^+) = \left\{ W(X_{\pi^+}) P'_{\pi^+} + \left[1 - W(X_{\pi^+}) \right] P_{\pi^+} \right\} d\sigma,$$

and similar formulae for $\bar{p}$ and $\pi^- : p \to \bar{p}$, $\pi^+ \to \pi^-$. The variables X_p and X_π are the scaled longitudinal momenta in the c.m.s. and the form of the weight function W used in our computation is

$$W(X) = \begin{cases} 0, & -1 \leqslant x < -\frac{1}{2}, \\ \frac{1}{2} + \frac{3}{2}x - 2x^3, & -\frac{1}{2} \leqslant x \leqslant \frac{1}{2}, \\ 1, & \frac{1}{2} < x \leqslant 1. \end{cases}$$

When this method is applied to a sample of about 80 000 inelastic events, the statistical error of the integrated proton, antiproton spectrum is about 0.95% and for the integrated π^+, π^- spectrum the error is about 0.3%. These are only about double the errors in the case where all the particles could be identified. This result is in agreement with that obtained in ref. [6].

References

[1] P.D. Gall, Thesis, DESY FI-76/02
[2] V. Blobel et al., Nucl. Phys. B69 (1974) 454; Phys. Lett. 48B (1974) 73
[3] H. Muirhead, CERN, 74-18 (1974) 488

[4] P.S. Gregory, University of Helsinki Report Series in Physics, No. 103 (1975) 256;
P.S. Gregory et al., Nucl. Phys. B143 (1978) 263
[5] D.B. Smith, R.J. Sprafka and J.A. Anderson, Phys. Rev. Lett. 28 (1969) 1064
[6] V. Idschok et al., Nucl Phys. B67 (1973) 93
[7] D. Bertrand et al., Nucl. Phys. B128 (1977) 365
[8] K. Jaeger et al., Phys. Rev. D11 (1975) 1756
[9] M. Markytan et al., Nucl. Phys. B143 (1978) 263
[10] J.F. Baland et al., Nucl. Phys. B140 (1978) 220
[11] R. Kinnunen et al., Amsterdam-Helsinki-Liverpool-Stockholm collaboration, preprint
[12] A.M. Cooper et al., Nucl. Phys. B136 (1978) 365
[13] R. Hamatsu et al., Nucl Phys. B123 (1977) 189;
C.K. Chen et al., Phys. Rev. D17 (1978) 42;
P. Gregory et al., Nucl. Phys. B143 (1978) 263;
D.I. Ermilova et al., Nucl. Phys. B137 (1978) 29;
R. Raja et al., Phys. Rev. D16 (1977) 2733
[14] V.V. Ammosov et al., Yad. Fiz 34 (1976) 59;
R. Singer et al., Phys. Lett. 60B (1976) 385,
H. Kichimi et al., Contribution to Tokyo Conf., 1978;
M.G. Albrow et al., Nucl. Phys. B155 (1979) 39
[15] A.M. Cooper et al, Nucl. Phys. B136 (1978) 365;
S. Banerjee et al., Contribution to Geneva Conf., 1979;
H. Kichimi et al., KEK preprint-78-10